Carbon−Silicon Hyperconjugation and Strain-Enhanced Hyperconjugation: Structures of *N*-Methyl 2- and 4-*tert*-Butyldimethylsilylmethyl Pyridinium Cations

Kathryn Hassall, Sofia Lobachevsky, Carl H. Schiesser, and Jonathan M. White*

School of Chemistry and the BIO-21 Institute, The University of Melbourne, Victoria 3010, Australia

Received October 12, 2006

NBO analysis of the interaction of trialkylsilylmethyl substituents with the electron-deficient pyridinium cation suggests that hyperconjugation is strongest at the 2-position. Crystal structures of 2- and 4-*tert*-butyldimethylsilylmethyl-substituted *N*-methyl pyridinium cations **2d** and **3d** however do not reveal any significant structural differences arising from differences in hyperconjugation at the 2- and 4-positions. Previously observed differences in the triisopropylsilyl derivatives **2c** and **3c** are proposed to arise as a result of strain-enhanced hyperconjugation.

Introduction

The stabilizing interaction between a C−Si bond and an electron-deficient center at the β-position is well established,[1] known as the silicon β-effect, the origin of which is strong hyperconjugation between the high-lying and polarized C−Si bond and a low-lying, vacant orbital at the β-position (Figure 1).[2] Stabilization energies for 1°, 2°, and 3° carbenium ions have been calculated from the appropriate isodesmic equations and give values of 38, 28, and 18 kcal/mol, respectively, showing that the magnitude of the silicon β-effect depends on the electron demand of the cation.[3,4] Structurally the silicon β-effect manifests in lengthening of the C−Si bond and shortening of the $C_\alpha-C_\beta$ bond, reflecting contributions of the double-bond−no-bond resonance form (Figure 1). Lambert has demonstrated the influence of C−Si−π neutral hyperconjugation on *p*-substituted benzyltrimethylsilanes **1**. The $^{29}Si-^{13}CH_2$ coupling constant decreased along the series X = OMe > Me > H > CN, indicating the increasing importance of the resonance form **1′** as the electronegativity of the substituent X increases.[5]

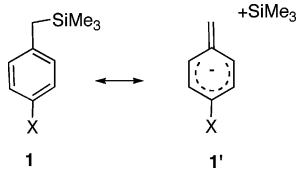

1 **1'**

Hyperconjugation in the charged silicon-substituted *N*-methyl pyridinium salts **2** and **3** has recently been demonstrated by a combination of X-ray crystallography and ^{29}Si and ^{13}C NMR spectroscopy.[6,7]

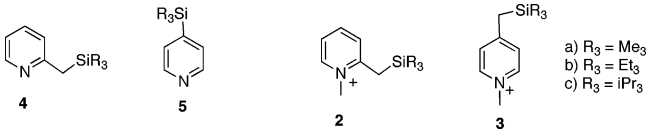

4 **5** **2** **3**

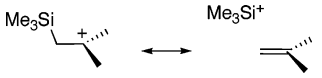

Figure 1.

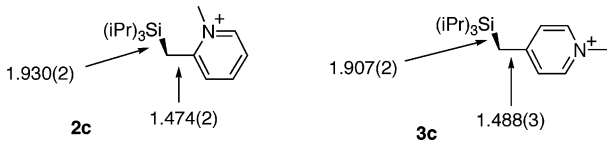

2c **3c**

Figure 2.

Upon methylation of the pyridine precursors **4** and **5**, a significant downfield shift in the ^{29}Si NMR spectrum was observed, accompanied by a decrease in the $^{13}C-^{29}Si$ one-bond coupling constant between the benzyl carbon and the R_3Si substituent, consistent with increased contributions of the double-bond−no-bond resonance forms **2′** and **3′** upon methylation.

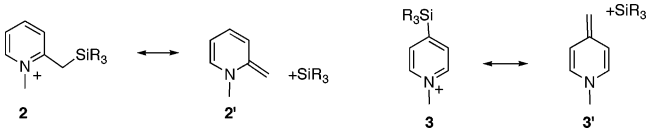

2 **2'** **3** **3'**

The magnitude of the effects in solution were found to be larger for the 2-trialkylsilylmethyl derivatives **2** than the 4-substituted derivatives **3**, leading to the conclusion that hyperconjugation is stronger at the 2-position of the pyridinium ion compared with the 4-position. This was supported by X-ray crystal structures of the 2- and 4-triisopropysilylmethyl derivatives **2c** and **3c**, whose structural parameters are summarized in Figure 2. Thus greater contributions of the resonance forms **2′** to the ground state structure of **2c** is implied by the longer CH_2-Si bond distance and the shorter $C(Ar)-CH_2$ distance.

This was surprising to us because simple Hückel calculations reveal that the coefficient of the LUMO of the pyridinium cation is larger at C4 than at C2[8] and would therefore be expected to

* Corresponding author. E-mail: whitejm@unimelb.edu.au.

(1) Lambert, J. B. *Tetrahedron* **1990**, *46*, 2677.
(2) White, J. M.; Clark, C. I. *Topics in Stereochemistry*; Denmark, S. E., Ed.; John Wiley and Sons: New York, 1999; Vol. 22, Chapter 3.
(3) Wierschke, S. G.; Chandrasekhai, J.; Jorgensen, W. L. *J. Am. Chem. Soc.* **1985**, *107*, 1496.
(4) Ibrahim, M. R.; Jorgensen, W. L. *J. Am. Chem. Soc.* **1989**, *111*, 819.
(5) Lambert, J. B.; Shawl, C. E.; Basso, E. *Can. J. Chem.* **2000**, *78*, 1441.
(6) Happer, A.; Ng, J.; Pool, B.; White, J. M. *J. Organomet. Chem.* **2002**, *659*, 10.
(7) Hassall, K.; Lobachevsky, S.; White, J. M. *J. Org. Chem.* **2005**, *70*, 1993.
(8) Fleming, I. *Frontier Orbitals and Organic Chemical Reactions*; John Wiley and Sons: New York, 1976.

10.1021/om060939e CCC: $37.00
Publication on Web 02/09/2007

interact more strongly with a C−Si bond attached at C4. This prompted us to carry out *ab initio* calculations on the 2- and 4-trimethylsilyl-substituted *N*-methyl pyridininium ions **2a** and **3a** to gain further insight into the nature of the interaction between the silicon substituent and the electron-deficient pyridinium ring.

Calculations were performed at the B3LYP/6-311G** level of theory,[9] and energies were ZPE corrected. Calculated structures with relevant structural parameters for the *N*-methyl 2- and 4-trimethylsilylmethyl pyridinium ions **2a** and **3a** are available in the Supporting Information. Stabilization energy resulting from interaction between the trimethylsilylmethyl substituents and the pyridinium cation is estimated from the calculated enthalpy changes in the isodesmic equations (eqs 1 and 2).

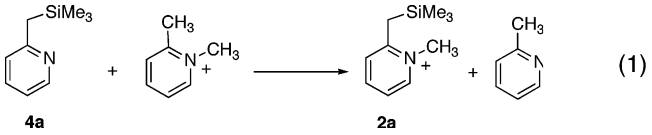

(1)

$\Delta E = -15.43$ kJ/mol (with zero-point correction)

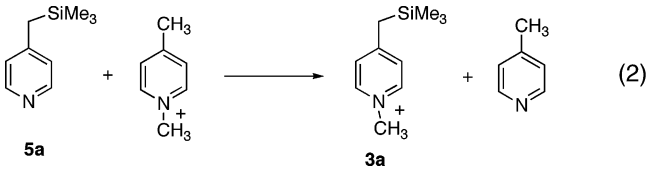

(2)

$\Delta E = -22.29$ kJ/mol (with zero-point correction)

The 4-substituted system (eq 2) is calculated to be 6.86 kJ/mol more exothermic than the 2-substituted system (eq 1). The greater enthalpy change associated with the formation of **3a** may suggest greater stabilization of this charged ion by the trimethylsilyl substituent compared to **2a**; however the effects of the steric interaction between the trimethylsilyl substituent and the *ortho*-*N*-methyl substituent need to be considered, as this would be expected to destabilize the right-hand side of eq 1. A better indicator of the strength of the $\sigma_{C-Si}-\pi$ interaction should be provided by NBO analysis[10,11] of the relevant interacting orbitals. Interaction energies between the σ_{C-Si} bond and the π system of the pyridinium ions **2a** and **3a**, which were determined by a second-order perturbation analysis, are presented in Table 1. These in fact do suggest a slightly stronger interaction between the trimethylsilyl substituent and the electron-deficient aromatic system in **2a** than in **3a**, although the structural effects associated with this stronger interaction are very small, with only slight lengthening of the C−Si bond in **2b** compared with **3b**. This result suggests that steric effects are likely to be important in the calculated enthalpy change in eq 2.

Table 1. NBO Interaction between the C−Si σ-Bond and the Aromatic π System in 2a and 3a

	NBO interaction (kJ/mol)	calculated C−Si bond distance (Å)
2a	52.3	1.966
3a	43.4	1.960

The X-ray structural data of the triisopropylsilyl derivatives **2c** and **3c** above suggest that the 2-triisopropylsilyl substituent interacts much more strongly with the aromatic ring system compared with the 4-triisopropylsilyl derivative than the above NBO analysis might suggest. The extra lengthening of the C−Si bond in **2c**, upon which this argument is based, may be due to a steric interaction between the *N*-methyl substituent and the isopropyl substituents on the silicon, this interaction being partially relieved by stretching of the C−Si bond. If this is the case, then why would the $C_{ipso}-CH_2$ bond (1.473 Å) also be shorter? We believe that the steric strain on the C−Si bond may be increasing its ability to participate in hyperconjugation. This phenomenon of "enhanced hyperconjugation" of strained bonds was first noted by Traylor for strained C−C bonds.[12] Hyperconjugation of strained carbon−carbon bonds has been more recently demonstrated in the crystal structures of a range of cyclopropylmethyl-substituted esters.[13]

To investigate whether the more pronounced structural effects of hyperconjugation in **2c** compared with **3c** arise due to steric effects in **2c**, it would be informative to compare the structures of the less sterically demanding trimethylsilyl derivatives **2a** and **3a**; however although the crystal structure of the 4-trimethylsilylmethyl-substituted derivative **3a** has been reported,[6] we found that the corresponding 2-substituted derivative **2a** desilylated during crystallization with a variety of counterions, so a comparison between the two structures could not be made. Given that desilylation of these species occurs by nucleophilic attack by the counterion at the silicon, we prepared the corresponding 2- and 4-(*tert*-butyldimethylsilyl)-substituted pyridinium cations **2d** and **3d**, for which this process would be disfavored.[14] The *tert*-butyldimethylsilyl substituent is considered less bulky than the triisopropylsilyl substituent in this context, as the *tert*-butyl group is able to position itself such that steric strain is minimized.

The pyridine derivatives **2d** and **3d** were prepared by methylation of the precursors **4d** and **5d**, which were prepared according to Scheme 1. Crystal data for **2d** and **3b** were measured at low temperature to minimize the unwanted effects of thermal motion. Crystal data and structure refinement details are summarized in Table 2, selected bond distances, angles, and dihedral angles are in Table 3, and perspective diagrams are presented in Figures 3 and 4, respectively. The conformation about the Si−C(6) bond places the *tert*-butyl group essentially *anti* with respect to the pyridinium ring (dihedral angles −163.2(2)° and −168.7(1)° for **2d** and **3d**, respectively); thus any steric effect should be minimal. In both structures the geometries about the silicon substituent are very similar, with C(Ar)−C(6)−Si bond angles that are essentially identical being close to normal. The silicon substituent is essentially orthogonal to the pyridinium ring in both structures, allowing for optimal overlap between

(9) Frisch, M. J.; Trucks, G. W.; Schlegel, H. B.; Scuseria, G. E.; Robb, M. A.; Cheeseman, J. R.; Montgomery, J. A., Jr.; Vreven, T.; Kudin, K. N.; Burant, J. C.; Millam, J. M.; Iyenger, S. S.; Tomasi, J.; Barone, V.; Mennucci, B.; Cossi, M.; Scalmani, G.; Rega, N.; Petersson, G. A.; Nakatsuji, H.; Hada, M.; Ehara, M.; Toyota, K.; Fukuda, R.; Hasegawa, J.; Ishida, M.; Nakajima, T.; Honda, Y.; Kitao, O.; Nakai, H.; Klene, M.; Li, X.; Knox, J. E.; Hratchian, H. P.; Cross, J. B.; Adamo, C.; Jaramillo, J.; Gomperts, R.; Stratmann, R. E.; Yazyev, O.; Austin, A. J.; Cammi, R.; Pomelli, C.; Ochterski, J. W.; Ayala, P. Y.; Morokuma, K.; Voth, G. A.; Salvador, P.; Dannenberg, J. J.; Zakrzewski, V. G.; Dapprich, S.; Daniels, A. D.; Strain, M. C.; Farkas, O.; Malick, D. K.; Rabuck, A. D.; Raghavachari; Foresman, J. B.; Ortiz, J. V.; Cui, Q.; Baboul, A. G.; Clifford, S.; Cioslowski, J.; Stefanov, B. B.; Liu, G.; Liashenko, A.; Piskorz, P.; Komaromi, I.; Martin, R. L.; Fox, D. J.; Keith, T.; Al-Laham, M. A.; Peng, C. Y.; Nanayakkara, A.; Challacombe, M.; Gill, P. M. W.; Johnson, B.; Chen, W.; Wong, M. W.; Gonzalez, C.; Pople, J. A. *Gaussian 03, Revision B.04*; Gaussian, Inc.: Pittsburgh, PA, 2003.

(10) Glendening, E. D.; Badenhoop, J. K.; Reed, A. E.; Carpenter, J. E.; Weinhold, F. *NBO*, 4.0; University of Wisconsin: Madison, WI, 1996.

(11) Reed, A. E.; Curtiss, L. A.; Weinhold, F. *Chem. Rev.* **1988**, *88*, 899.

(12) Clinton, N. A.; Brown, R. S.; Traylor, T. G. *J. Am. Chem. Soc.* **1970**, *92*, 5228.

(13) White, J. M.; Fifer, N. *Org. Biomol. Chem.* **2005**, 1776.

(14) Lew, S. Q.; McClelland, R. A. *J. Am. Chem. Soc.* **1993**, *115*, 11516.

Scheme 1[a]

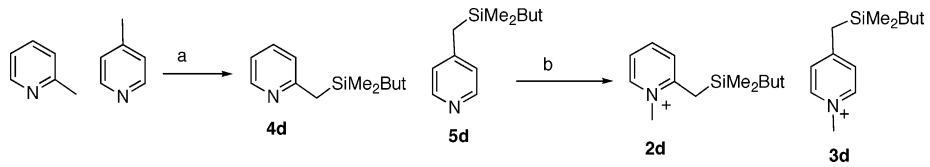

[a] (a) MeLi/Et_2O, then $ButMe_2SiCl$; (b) $Me-OSO_2CF_3$.

Table 2. Crystal Data and Structure Refinement Details for Pyridinium Ions 2d and 3d

	2d	3d
empirical formula	$C_{14}H_{24}F_3NO_3SSi$	$C_{14}H_{24}F_3NO_3SSi$
fw	371.49	371.49
temperature (K)	130.0(1)	130.0(1)
radiation	Mo Kα	Mo Ka
wavelength (Å)	0.71073	0.71073
cryst syst	triclinic	orthorhombic
space group	$P\bar{1}$	*Pbca*
unit cell dimens		
a (Å)	7.5246(10)	10.7340(5)
b (Å)	7.9937(11)	11.2427(5)
c (Å)	16.031(2)	31.3159(15)
α (deg)	102.489(3)	
β (deg)	98.539(2)	
γ (deg)	91.521(2)	
volume (Å^3)	929.3(2)	3779.2(3)
Z	2	8
D_c (Mg/m^3)	1.328	1.306
μ (mm^{-1})	0.278	0.273
F(000)	392	1568
cryst size (mm)	0.50 × 0.10 × 0.05	0.50 × 0.40 × 0.30
θ range (deg)	1.32 to 25.00	2.30 to 25.00
no. of reflns collected	4908	18 612
no. of indep reflns	3220	3332
R(int)	0.0435	0.0510
obsd reflns ($I > 2\sigma(I)$)	2201	2983
no. of data/restraints/ params	3220/0/214	3332/0/215
GOF on F^2	0.912	1.072
final *R* indices [$I > 2\sigma(I)$]	0.0492	0.0396
	wR2 = 0.0969	wR2 = 0.1054
R indices (all data)	0.0742	0.0435
	wR2 = 0.1031	wR2 = 0.1078
weighting scheme[a]	$A = 0.0366$	$A = 0.0616$
	$B = 0$	B = 1.12
extinction coeff	0.0003(6)	0.0012(2)
largest diff peak and hole (e Å^{-3})	0.582 and −0.266	0.349 and −0.234

[a] $w = 1/[\sigma^2(F_o^2) + (AP)^2 + BP]$; where $P = (F_o^2 + 2F_c^2)/3$.

Table 3. Selected Bond Distances (Å), Angles (deg), and Dihedral Angles (deg) for Ions 2d and 3d

	2d	3d
C(1)−N(1)	1.356(3)	1.342(2)
C(1)−C(2)	1.390(4)	1.363(3)
C(2)−C(3)	1.375(4)	1.402(3)
C(3)−C(4)	1.382(4)	1.400(3)
C(4)−C(5)	1.366(4)	1.364(3)
C(5)−N(1)	1.356(3)	1.345(2)
C(6)−C(Ar)	1.484(3)	1.480(3)
C(6)−Si(1)	1.919(3)	1.916(2)
C(7)−Si(1)	1.870(3)	1.862(2)
C(8)−Si(1)	1.860(3)	1.864(2)
C(9)−Si(1)	1.885(3)	1.895(2)
C(Ar)−C(6)−Si(1)	111.43(18)	111.33(12)
N(1)−C(1)−C(6)−Si(1)	94.4(3)	
C(2)−C(1)−C(6)−Si(1)	−81.7(3)	
C(1)−C(6)−Si(1)−C(9)	−163.2(2)	
C(4)−C(3)−C(6)−Si		−88.82(19)
C(2)−C(3)−C(6)−Si		88.14(19)
C(3)−C(6)−Si−C(9)		−168.7(1)

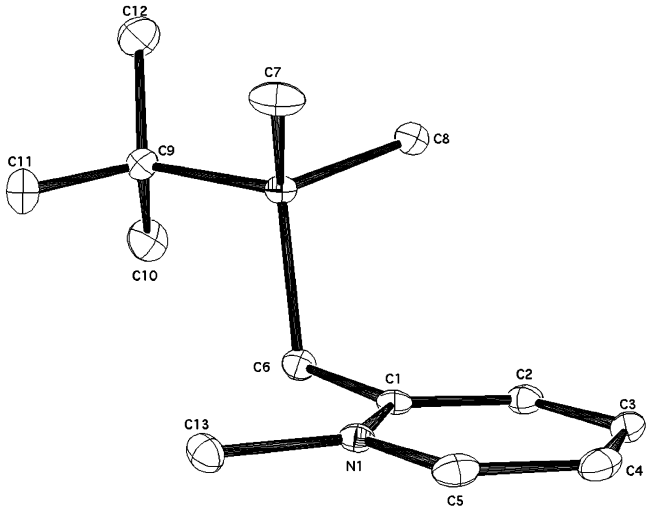

Figure 3. Thermal ellipsoid plot of cation **2a**. Ellipsoids are at the 20% probability level.

the C(6)−Si σ bond and the aromatic π system. Consistent with this, the Si−C(6) bond distance in both structures is significantly longer than the other Si−C bonds that are not involved in this hyperconjugative interaction. Comparison between the Si−C(6) and C(6)−C(Ar) distances for the two structures **2d** and **3d** reveals no significant differences between them, suggesting that the structural effects of hyperconjugation are similar. This contrasts with the previous result for the triisopropylsilyl-substituted derivatives **2c** and **3c**, but is in qualitative agreement with the calculated structures **2a** and **3a**. Thus there is no structural evidence to suggest that hyperconjugation is stronger at the 2-position of the pyridinium cation compared with the 4-position, although NBO analysis suggests that there is a difference; the difference must be too small for it to be detectable using X-ray crystallography.

Experimental Section

X-ray Crystallography. Crystals of **2d** and **3d** were grown from acetonitrile. The temperature during data collection was maintained at 130.0(1) K using an Oxford Cryostream cooling device. Intensity data were collected with a Bruker SMART Apex CCD detector using Mo Kα radiation (graphite crystal monochromator λ = 0.71073). Data were reduced using the program SAINT.[15]

The structure was solved by direct methods and difference Fourier synthesis. Thermal ellipsoid plots were generated using the program ORTEP-3[16] integrated within the WINGX[17] suite of programs.

Computational Procedures. All calculations were performed using the Gaussian 03 program. Geometries were fully optimized at B3LYP/6-311G(2d,p) without constraints, and these energies were further improved by addition of unscaled zero-point vibrational energy differences (ΔZPVE) (B3LYP/6-311G(2d,p) + ΔZPVE). (Calculations were initially performed at varying levels of theory

(15) *SMART*, *SAINT*, *SADABS*; Siemens Analytical X-ray Instruments Inc.: Madison, WI, 1999.
(16) Farrugia, L. J. *J. Appl. Crystallogr.* **1997**, *30*, 565.
(17) Farrugia, L. J. *J. Appl. Crystallogr.* **1999**, *32*, 837.

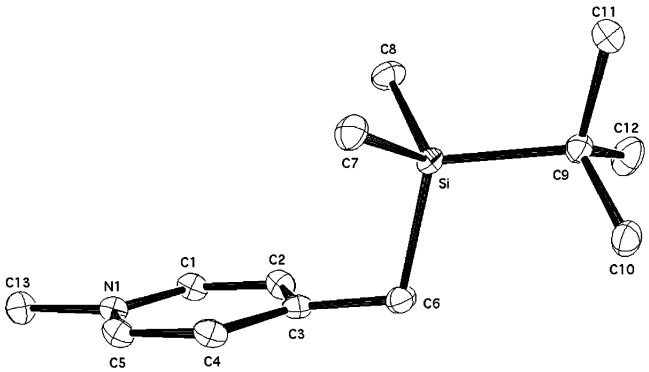

Figure 4. Thermal ellipsoid plot of cation **3a**. Ellipsoids are at the 20% probability level.

and basis sets, from RHF/3-21G(*) up to MP2/6-311G**. We found that B3LYP/6-311G** gave results that were comparable with MP2/6-311G** for significantly less computing time.) NBO analysis was performed without orbital deletions and therefore represents a second-order perturbation analysis. A full listing of geometries and energies (Gaussian Archive entries) of structures studied is provided in the Supporting Information.

Synthesis. General experimental details are published elsewhere.[7]

***N*-Methyl 2-*tert*-Butyldimethylsilylmethylpyridinium Triflate, [2d]$^+$[triflate]$^-$.** A solution of **4d** (100 mg) in deuteroacetonitrile (0.5 mL) was treated with neat methyl triflate (1.05 equiv). After the NMR had been recorded, ether was allowed to diffuse into the solution overnight to afford colorless plates suitable for X-ray analysis. ^{1}H NMR (400 MHz, CD_3CN): δ 8.51 (1H, dd, J = 6.4 Hz, H6), 8.24 (1H, dd, J = 7.4,7.4 Hz, H4), 7.68 (1H, d, J = 8.2 Hz, H3), 7.64 (1H, d, J = 7.0 Hz, H5), 4.11 (3H, s, N$-CH_3$)$_2$, 2.77 (2H, s, CH_2), 1.03 (9H, s, Si$-C(CH_3)_3$), 0.04 (6H, s, Si$-CH_3$). ^{13}C NMR (100 MHz, CD_3CN): δ 161.7 (C2), 146.8 (C6), 145.1 (C4), 129.5 (C5), 124.3 (C3), 47.0 (N$-CH_3$), 26.5 (Si$-C(CH_3)_3$), 23.1 (CH_2, $^1J_{C-Si}$ = 33.0 Hz), 17.8 (Si$-C(CH_3)_3$, $^1J_{C-Si}$ = 58.7 Hz), $-$5.62 (Si$-CH_3$, $^1J_{C-Si}$ = 51.9 Hz). ^{29}Si NMR (80 MHz, CD_3CN): δ 18.49.

4-*tert*-Butyldimethylsilylmethylpyridine (5d). To a solution of 4-picoline (2.01 g, 21 mmol) in ether (20 mL) was added methyl lithium (1.4 M in ether, 15 mL, 21 mmol) and the solution refluxed for 30 min. The reaction was cooled to $-$78 °C (dry ice/acetone) prior to the dropwise addition of a solution of *tert*-butyldimethylsilyl chloride (3.77 g, 25 mmol) in ether (5 mL). The mixture was slowly warmed to room temperature and stirred for a further 3 h. The product was extracted with 1 M HCl (2 × 50 mL) and washed with ether (50 mL). The aqueous layer was made basic (pH 12) with concentrated NaOH solution and the product extracted with ether (3 × 50 mL). The combined ether layers were dried ($MgSO_4$), and the solvent was removed under reduced pressure to afford an orange oil (4.015 g, 92%). ^{1}H NMR (400 MHz, $CDCl_3$): δ 8.37 (2H, d, J = 5.8 Hz, H2/6), 6.92 (2H, d, J = 4.5 Hz, H3/5), 2.09 (2H, s, CH_2), 0.90 (9H, s, Si$-C(CH_3)_3$), $-$0.11 (6H, s, Si$-CH_3$). ^{13}C NMR (100 MHz, $CDCl_3$): δ 150.38 (C4), 149.1 (C2/6), 123.6 (C3/5), 26.3 (Si$-C(CH_3)_3$), 22.8 (CH_2, $^1J_{C-Si}$ = 41.9 Hz), 16.6 (Si$-C(CH_3)_3$, $^1J_{C-Si}$ = 56.5 Hz), $-$6.80 (Si$-CH_3$, $^1J_{C-Si}$ = 51.1 Hz). ^{29}Si NMR (80 MHz, $CDCl_3$): δ 8.77. ESI-MS (*m/z*): 208.1 [M + H]$^+$.

2-*tert*-Butyldimethylsilylmethylpyridine (4d). The same general procedure for the preparation of **5d** was employed, giving **4d** as a yellow oil (49% yield). ^{1}H NMR (400 MHz, $CDCl_3$): δ 8.34 (1H, dd, J = 4.9, 1.6 Hz, H6), 7.42 (1H, ddd, J = 7.7, 7.7, 1.7 Hz, H4), 6.89 (2H, m, H3/5), 2.28 (2H, s, CH_2), 0.84 (9H, s, Si$-C(CH_3)_3$), $-$0.18 (6H, s, Si$-CH_3$). ^{13}C NMR (100 MHz, $CDCl_3$): δ 161.4 (C2), 148.6 (C6), 135.7 (C4), 122.3 (C5), 119.0 (C3), 26.3 (Si$-C(CH_3)_3$), 25.8 (CH_2, $^1J_{C-Si}$ = 42.7 Hz), 16.6 (Si$-C(CH_3)_3$, $^1J_{C-Si}$ = 56.5 Hz), $-$6.50 (Si$-CH_3$, $^1J_{C-Si}$ = 51.1 Hz). ^{29}Si NMR (80 MHz, $CDCl_3$): δ 9.09. ESI-MS (*m/z*): 208.1 [M + H]$^+$.

***N*-Methyl 4-*tert*-Butyldimethylsilylmethylpyridinium Triflate, [3d]$^+$[triflate]$^-$.** A solution of **5d** (100 mg) in deuteroacetonitrile (0.5 mL) was treated with neat methyl triflate (1.05 equiv). X-ray quality crystals were obtained from slow evaporation of solvent. ^{1}H NMR (400 MHz, CD_3CN): δ 8.43 (2H, d, J = 5.9 Hz, H2/6), 7.61 (2H, d, J = 6.1 Hz, H3/5), 4.20 (3H, s, N$-CH_3$), 2.57 (2H, s, CH_2), 0.94 (9H, s, Si$-C(CH_3)_3$), $-$0.07 (6H, s, Si$-CH_3$). ^{13}C NMR (100 MHz, CD_3CN): δ 164.8 (C4), 144.7 (C2/6), 127.6 (C3/5), 47.8 (N$-CH_3$), 26.8 (Si$-C(CH_3)_3$), 26.6 (CH_2, $^1J_{C-Si}$ = 33.6 Hz), 17.8 (Si$-C(CH_3)_3$, $^1J_{C-Si}$ = 58.0 Hz), $-$6.50 (Si$-CH_3$, $^1J_{C-Si}$ = 52.6 Hz). ^{29}Si NMR (80 MHz, CD_3CN): δ 16.85.

Crystallographic data supplied in CIF format have been deposited with the Cambridge Crystallographic Data Centre, CCDC reference numbers 631422 and 631423.

Acknowledgment. Ours thanks go to the University of Melbourne MRDGS scheme for financial support and to Australian Research Council for the award of an APRA (K.H.).

Supporting Information Available: A full listing of geometries and energies (Gaussian Archive entries) of structures studied are provided. This material is available free of charge via the Internet at http://pubs.acs.org.

OM060939E